Latin American Journal of Solids and Structures
www.lajss.org

Structural Behavior of RC Beams Containing a Pre- Diagonal Tension Crack

Abstract
This study focuses the light on the shear behavior of pre-cracked beams, and examines the feasibility of applying fracture mechanics concepts to widen the understanding of shear behavior and mechanisms. The experimental program contains ten beam specimens of high strength concrete (HSC) and steel fiber reinforced concrete (SFRC). Pre-cracks were embedded with different sizes and locations along the favorable path and orientation to shear failure. Three main scenarios of shear failure were reported with minute effect of pre-cracks. The geometrical effect is dominant with marginal effect of the material's nonlinearity in case of severe pre-diagonal crack in HSC while the nonlinearity of the material is supreme to that of the geometrical effect for SFRC and shorter cracks. For verification, numerical simulation was conducted to examine the geometrical effect of the pre-diagonal tension crack in shear span on the structural behavior of RC beams. It is found numerically that, when the crack tip of the tensile crack is away from the tensile reinforcement, the closuring moment of tensile reinforcement increases, and as a result reduces the strain energy release rate. Therefore, the tensile cracks stop and the shear cracks keep propagating leading the failure mechanism to the end failure point.

Keywords
High strength concrete; fiber reinforced concrete; diagonal tension crack; shear strength; fracture mechanics; finite element analysis.

H.S.S Abou El-Mal[a]
A.S. Sherbini[b]
H.E.M Sallam[c]*

[a] Civil Engineering Departament, Jazan University, Jazan, KSA, Menofia University, Shibin El-Kom, Egypt.
E-mail: heshnan@yahoo.com

[b] Civil Engineering Departament, Jazan University, Jazan, KSA., Suez Canal University, Ismailya, Egypt.
E-mail: amrsukr@yahoo.com

[c] Civil Engineering Departament, Jazan University, Jazan, KSA, Zagazig University, Zagazig, Egypt.
E-mail: hem_sallam@yahoo.com

*Corresponding author

http://dx.doi.org/10.1590/1679-78254701

Received: November 27, 2017
In Revised Form: February 28, 2018
Accepted: March 27, 2018
Available Online: April 11, 2018

1 INTRODUCTION

Shear behavior of reinforced concrete (RC) beams is still not clearly understood due to its complexity. The numerous interacting parameters such as, concrete strength and composition, longitudinal steel ratio, shear span-depth ratio (a/d), and the vertical web reinforcement made the explanation of shear failure mechanisms barely aceptable, Coccia et al (2015); Caldentey et al (2013). Despite several decades of experimental investigations on the shear behavior of RC beams, worldwide practical design codes for predicting the shear capacity of RC beams are still empirically expressed. ACI Committee 318 (2005); BS 8110 (1997); CSA Committee A23.3 (1994).

The developed methods of RC shear design remain mostly unchanged. Compression field theory (Collins 1978); modified compression field theory, Vecchio and Collins (1986); strut and tie model, Schlaich et al (1987) and the concept of 'compressive-force path' (CFP) Kotsovos (1988) have evolved in the general field of structural concrete design. Most of these methods minutely deviate from the basis on which present-day design is founded; and still carrying implicit assumptions which, in many cases, are incompatible with the fundamental properties of concrete.

The effect of concretes compositions and strength on the shear behavior of RC beams was investigated by Chiu et al (2016); Resende et al (2016); Sagaseta (2013). Lim and Hong (2016) studied the shear behavior of ultra-high performance fiber reinforced concrete (UHPFRC) rectangular cross sectional beams with fiber volume fraction of 1.5% considering a spacing of shear reinforcement. They found that, the shear strength of the beams with shear reinforcement was larger than that of control specimen and was improved about 13–19%. In addition, the steel fibers in UHPFRC beam play a key role to restrain the shear crack along with the shear reinforcement. Concrete structures by default are full of cracks, and the idea of applying the stress intensity factors to design of concrete might be the third major revolution in design after the development of elastic no tension analysis and the introduction of plastic limit analysis. The ACI fracture mechanics of concrete committee 446, ACI 446.1R-91

(ACI Committee Reports, 1999) reported that, the theory formulated mostly during the last decades finally appears to be ripe. Fracture researchers have at the present no doubt that the introduction of fracture mechanics into the design criteria for all brittle failures of reinforced concrete structures (such as diagonal shear, punching shear, and torsion), can bring about significant benefits. It will make it possible to achieve more uniform safety margins, especially for structures of different sizes. This, in turn, will improve economy as well as structural reliability. It will make it possible to introduce new designs and utilize new concrete materials. Fracture mechanics will be particularly important for high strength concrete structures, fiber-reinforced concrete structures, and concrete structures of unusually large sizes, ACI 446.1R-91 (ACI Committee Reports, 1999). The field of fracture mechanics deals with the prediction of crack propagation in structures, which could be applied to deepen the understanding of shear failure mechanisms.

The fracture mechanics approach was first considered by Reinhardt (1981) to account for the size effect in shear strength. Since then, many researchers started to attempt to analyze the shear behavior of RC beams using the concept of fracture mechanics. Bažant developed a size effect formula from fracture mechanics for predicting the shear strength, Bažant (1984). Then, Bažant and Kim further studied the size effect on the shear capacity of RC beams without stirrups using the size effect approach, considering the common contribution of the arch action and the beam action to the shear capacity, Bažant and Kim (1984). The size effect formula was extended by Bažant with the consideration of the cohesive stresses across the diagonal shear crack, Bažant (1987). Later, Gustafsson and Hillerborg numerically studied the diagonal shear cracking processes in RC members using the fictitious crack model, Gustafsson and Hillerborg (1988). In 2003, Bažant and Yu presented a new formula to consider the size effect of the shear capacity of RC members, Bažant and Yu (2005).

The shear failure mechanisms of RC members were investigated by Jenq and Shah (1989) using the two-parameter fracture model. Later, So and Karihaloo (1993) made a modification to Jenq and Shah's model through taking into account the dowel action and the aggregate interlock in addition to considering the bond-slip relationship. Gastebled and May proposed a new analytical model for the flexural shear failure of RC beams using the fracture energy approach, Gastebled and May (2001). Carpinteri et. al. (2011) predicted the three collapse mechanisms, i.e. flexure, shear, and crushing, of RC beams using a fracture mechanics model. Bykov et. al. (2015) found that, the leading role in the evolution of the crack formation process is played by the mechanism of fracture of bonds between the reinforcing elements and the concrete.

Fracture mechanics concepts were successfully applied on propagating cracks under mode I (opening mode). Sallam et al (2004) proved that, the behavior of pre-cracked specimen is identical to that of smooth specimen when the generated crack in the smooth specimen reaches an equal length as that of the pre-cracked one. The behavior of both specimens is different at the stage before generating the first crack till it reaches the pre crack length. A similar finding was reported by Yehia and Wahab (2007) regarding T-flanged reinforced concrete beams.

Cracks may be unimportant to the continued functioning of the structure or they may run catastrophically causing great damage to property and life. The most favorable site of diagonal tension crack initiation in both normal and fiber reinforced concrete has been proposed by Abou El Mal et al (2015a) to monitor shear mechanisms in the presence of unstable pre-cracks. Earlier experimental investigations have highlighted that the incorporation of an adequate amount of steel fibers (1-2%) into the concrete matrix significantly improves the shear and flexural strength, ductility, and energy-absorbing capacity of SFRC flexural members, Sallam et al (2014).

Further study, however, is required to investigate the shear failure behavior of the SFRC for the various positions and sizes of triggering shear cracks along the favorable orientation. The current study is a trial to focus the light on the shear behavior of pre-cracked beams. The main objectives of this study are: 1) to evaluate the effect of position and size of shear cracks on the shear and flexural behavior, failure mode, crack propagation, and ductility of RC beams and 2) to examine the feasibility of applying fracture mechanics approach as a tool to understand shear failure process.

2 EXPERIMENTAL PROGRAM

An experimental program was designed to accomplish the objective of this work. Ten beam specimens were tested under static loads for various combinations of cracks sizes and positions. Two main groups of beams regarding the concrete type, i.e. HSC and SFRC, were investigated under the same variables. All tested beams were kept the same in concrete dimensions, longitudinal rebars (tension, compression), and stirrups alignment as shown in table1. Standard cylinders were prepared to measure the concrete compressive and indirect tensile

strengths. The details of specimens, test setup, instrumentations, materials used, and results of material testing are discussed in the following sections.

Table 1: *Details of test program*

Specimen	Fibers	Pre-Crack		Materials Proprieties (MPa)		Testing Results			
						Shear Capacity			Failure Scenario
	Vf %	Length (mm)	Position	Concrete comp. str.	Rebars yield str.	V_{LC}(kN)*	$V_{u,exp}$(kN)	$V_{LC}/V_{u,exp}$	
Series I (H.S.C)									
P_o	---	---	---	74.0	400	107	135	0.792	---
$P5_C$	---	50	Centered	"	"	99	"	0.733	I_{st}
$P5_{SH}$	---	50	Below N.A.	"	"	96	"	0.711	I_{st}
$P_{2.5C}$	---	25	Centered	"	"	103	"	0.763	II_{nd}
$P_{2.5SH}$	---	25	Below N.A.	"	"	98	"	0.726	II_{nd}
SeriesII (F.R.C)									
F_o	1.5	---	---	69	"	150	190	0.789	---
$F5_C$	1.5	50	Centered	"	"	142	"	0.747	II_{nd}
$F5_{SH}$	1.5	50	Below N.A.	"	"	140	"	0.736	II_{nd}
$F_{2.5C}$	1.5	25	Centered	"	"	146	"	0.768	III_{rd}
$F_{2.5SH}$	1.5	25	Below N.A.	"	"	143	"	0.752	III_{rd}

*V_{LC} = Capacity at Leading Crack

2.1 Details of test specimens

The beam test specimen adopted in this study represents a medium scale prototype of most commonly used beams. The width (w) and height (h) of all specimens were 150 and 250 mm, respectively, and the overall length was 2000 mm. Adopting Kani (1964, 1966) Valley theory a/d for current work was kept equal to 2.814. The critical (a/d)c for such configuration to force diagonal tension cracks equals 2.39. A clear concrete cover of 25 mm to the longitudinal and transverse steel was used in the specimens. All specimens had deficient shear stirrups throughout their lengths (1@400mm). The spacing between stirrups is almost 1.78 times the effective depth of beam (d) to promote shear failure mechanisms. The favorable site of pre cracks is targeted to be crossed by a stirrup; while the rest of generated cracks through the length of tested beam might propagate without being crossed by stirrups. Well designed flexural reinforcement (bottom reinforcement 3 Dia 16) accompanied with the deficient shear reinforcement guaranteed such shear failure mechanism, ACI Committee 318 (2005); BS 8110 (1997); CSA Committee A23.3 (1994). Reinforcement steel bars with yield strength of 400 MPa caging was designed to achieve high flexural strength (bottom reinforcement 3 Dia 16), and (upper reinforcement 2 Dia 16) connected with (stirrups 2.5 Dia 8 /m). All specimens were examined under four point bending as shown in Fig. 1. The pre cracks were developed using strips of rubber latex membrane with different width fitted to the form work of casted beams prior to casting at the targeted position according to the selected variables of the experimental study.

The steel reinforcement was instrumented using three strain gages on the bottom reinforcement and one strain gage on stirrup facing the pre crack prior to concrete casting as shown in Fig. 2. A full protocol of preparing reinforcement bars prior to installing the strain gages was carried out, the ribs of the bars were sanded by grinding where needed and the bar surface was cleaned with Ethanol and acidic conditioner. The surface was then cleansed with a neutralizer solution. The strain gages were attached to the bars using special cement recommended by the manufacturer. Electrical wires were soldered to the ends of the strain gages and attached to electrical terminals placed along the steel bar. The wires were then projected outside the steel cage at different locations. The strain gages and the terminals were covered with wax to protect the gages from damage during the concrete casting. Strain gages were also attached to the concrete surface at the mid span of the compression side (upper fiber) as shown in Fig. 2. All beams were tested using a computer controlled actuator with a capacity of 440 kN and a data acquisition system recording the readings of load cell, strain gages, and LVDTs.

Standard cylinders of size 100 x 200 mm were prepared to measure the concrete compressive and indirect tensile strengths as per ACI Standards ACI 318. A total of eighteen cylinders were prepared for each supplied batch. A nine cylinders sample is provided for each compressive or tensile strength test.

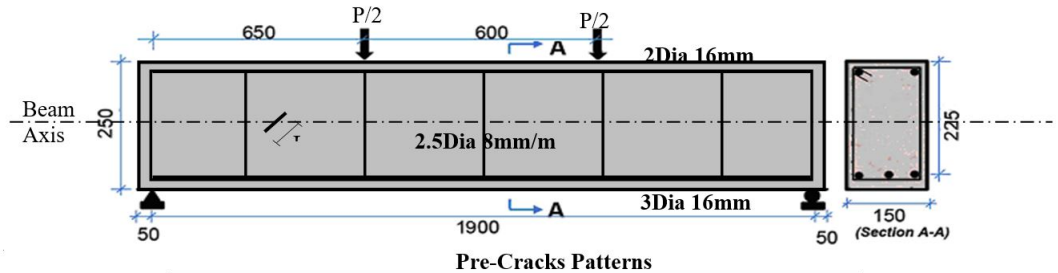

Pre-Cracks Patterns

Crack Length (L)	Position	Notation
5 cm	Centered with beam axis	5C
	Below beam axis	5SH
2.5 cm	Centered with beam axis	2.5C
	Below beam axis	2.5SH

Figure 1: *Dimensions, Positions and patterns of Pre-Cracks, and reinforcement detailing*

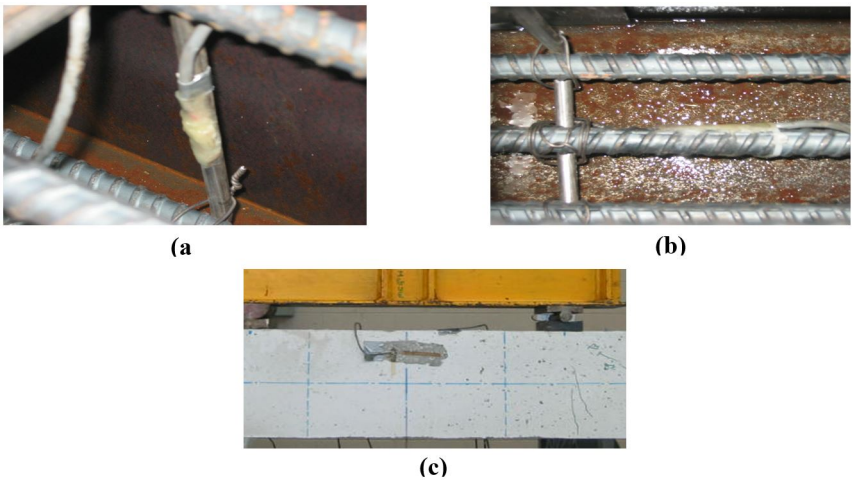

Figure 2: *Strain gauges fitting on stirrups (a), tension reinforcement (b),and concrete surface (c)*

2.1 Materials used

The concrete used in this test program is a high strength, self compacting, ready mix concrete. The average tested compressive strength of the concrete was 74 MPa and its tensile strength was 8 MPa. Steel fibers (hooked end RL- 45/50-BN DRAMIX steel fiber) with mechanical properties shown in table 2 were added with a volume fraction of 1.5% (V_f =0.015) on site at the conveying truck mixer when needed for fiber reinforced concrete beams fabrication.

Table 2: *DRAMIX Data Sheet*

Geometry	Length (L)	Performance	Aspect Ratio	Diameter
	45/50.0 mm	Class:45	L/d = 48	1.05 mm
Specifications	Tensile Strength	Coating	Carbon content	#/kg
	1000 N/mm²	None	Low Carbon	2800fibers/kg
DRAMIX **RL- 45/50-BN** (R_{ound}-L_{oose} Class 45-50mm B_{right}-$_{low\ carbo}$N)				

2.3 Test setup and instrumentation

A four point bending test was adopted for all beams in the current study. The load was applied using a computer controlled central actuator of 1.5 mm per minute stroke controlled system distributing its load through a stiff spreader beam to two points of load spacing 650 mm from the edge of beam and 600 mm from each other as shown in Fig. 1. A couple of virgin RC beams of both steel fiber reinforced concrete matrix SFRC, plain high strength concrete matrix HSC with no pre-cracks were cast and tested under the proposed configuration to work as a control group demonstrating the behavior of smooth specimen. Four couples of RC beams of both types of concrete with one sided pre-crack along the favorable site and orientation proposed by Abou El Mal et al were cast and tested under the same configuration.

In a trial to achieve the research goal, two different lengths of pre-cracks (2.5, and 5.0 cm) were embedded in two different positions (centered and below the beam axis) as shown in Fig. 1. The selected crack lengths were greater than the maximum aggregate size (MAS = 20 mm) to ensure crack growth severity following the finding of Abou El-Mal et al. (2015b), that the ratio of maximum size of non damage defect zone to MAS should be less than unity. In accordance with the compliance method of notched beams proposed by Swartz et. al., notches were installed to the beam using 2.5 and 5.0 cm wide strips of natural rubber latex membrane of 0.5 mm thickness to create the pre-notch, then, a maximum load is selected to be less than 1/3 the expected failure load was cycled for three times to emanate a crack from the notch root, Swartz et al (1978).

3 RESULTS AND DISCUSSION

The two control uncracked beams, HSC beam denoted as (Po) and SFRC beam denoted as (Fo), were tested till failure. Both the crack path and propagation history were recorded. It is clear from Figures 3 and 4 that, the diffusion of flexural cracks mainly in the central flexural zone is totally different. In case of Po beam, small number of flexural cracks (4-5 cracks) were first monitored at 90 kN (first shear crack load).

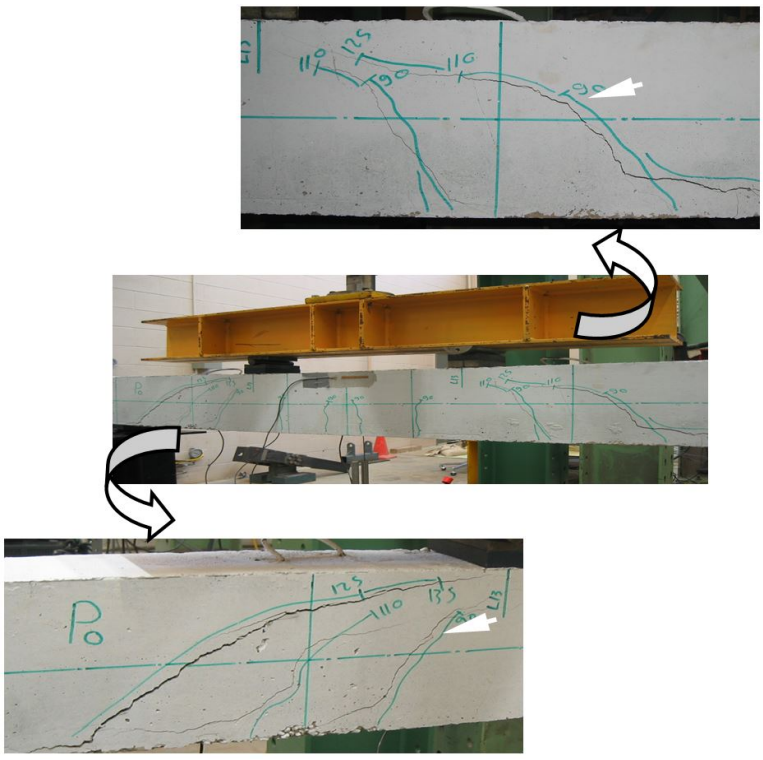

Figure 3: *Tracing Of Diagonal Tension Shear Crack Propagation in R.C Beams with HSC. Matrix.*

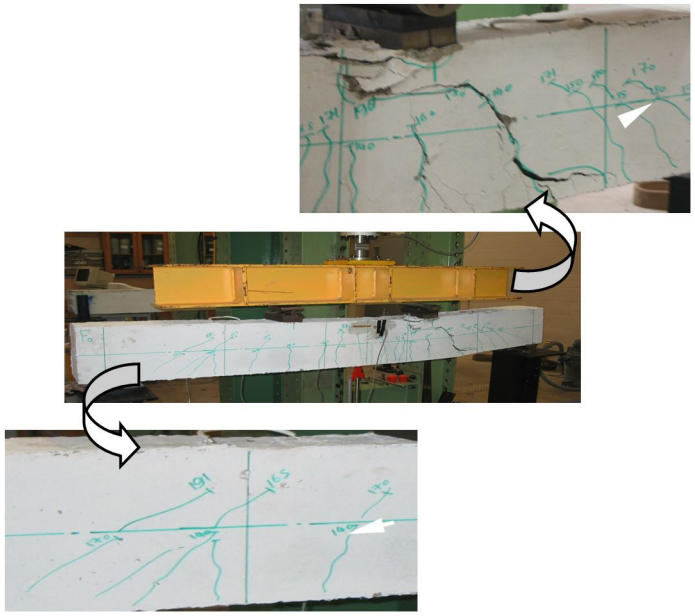

Figure 4: *Tracing Of Diagonal Tension Shear Crack Propagation in R.C Beams with SFRC. Matrix.*

In case of Fo beam, a higher diffusion of flexural cracks is obvious, more than 12 cracks in the same region were monitored at higher load level (140 kN), first shear crack load. Although the role of fibers is primarily in the post-cracking stage, the presence of fibers affected the first shear crack load in Fo beam. The presence of fibers embedded in concrete matrix might delay or arrest the flexural propagating cracks, consequently, other cracks might initiate at this load level. When the load level is increased some of the arrested cracks might propagate accompanied with newly initiated cracks. Due to numerous flexural cracks in case of Fo beam, the energy dissipated in this stage is higher than that of Po beam. Therefore, the wide difference of first shear crack load might be understood. Although the behavior of first monitored cracks was different between beams Po and Fo, the leading shear crack path and mode of failure at the end of test are almost identical.

The shear crack changed its propagation direction and kinked towards the point of loading at a load of 107 and 150 kN for Po and Fo respectively (Leading Crack). At this stage, multiple shear cracks are observed on both sides of the tested beam with almost the same pattern. The cracks continued to widen and increase in its length till a load of 125 and 170 kN for Po and Fo respectively. At a load of 135 and 190 kN for Po and Fo respectively the total failure occurred on one side of the beam. Due to the displacement controlled condition, the applied load decreased while the deflection of the beams and the width of shear cracks increased after reaching the failure load. On the other hand, all pre-cracked beams were tested till a leading shear crack is observed at almost from 70.0- 80.0% of the expected failure load as shown in table 1, then the test was terminated and the beams were kept un broken to be repaired in a subsequent study.

The most critical proposed pre-crack was the longer one (5.0cm) either centered with the beam axis denoted as (P5C) or totally located in the tension zone below the beam axis denoted as (P5SH). For those beams the plane of shear failure was forced to pass through the pre-crack then a main leading shear crack was achieved at almost from 70.0 - 80.0% of the expected failure load, at this stage, the path and behavior of the pre-cracked beam became identical to that of the control virgin beam as shown in Fig. 5.

Figure 5: *Main shear Coalesced crack with the pre-Crack*

From the previous pre-cracked tested beams, it was observed that, the first initiated and propagating crack is the tensile crack at zero shear, and constant Bending moment region. After that, another edge tensile crack

initiates at the shear span and propagates to coalesce with the pre- diagonal tension crack. By increasing the applied load, the coalesced crack will propagate till failure point, as shown in Fig.6. A similar behavior was observed by (Sallam et al 2004; Yehia and Wahab 2007) for pre-cracked Reinforced concrete beams under mode I, at which, the pre-crack propagated at a load equal to that of smooth specimens at the same crack length.

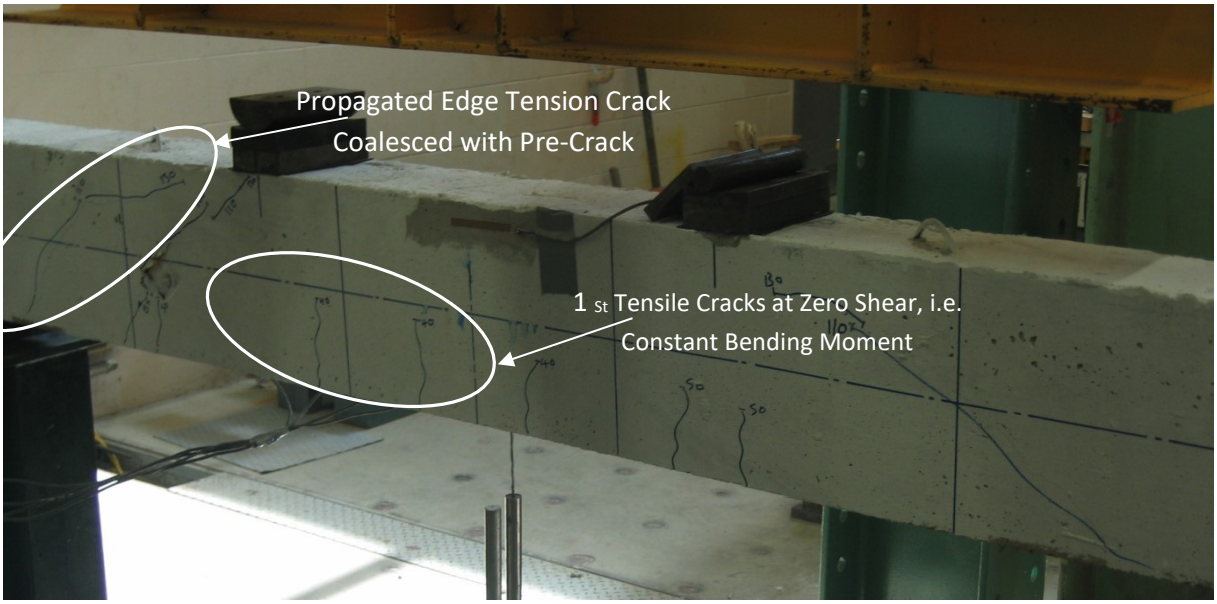

Figure 6: *Cracking of (P5C) Beam*

Due to the severity of pre diagonal crack, (5.0 cm) in plain concrete, the geometrical effect is dominant with marginal effect of the material's nonlinearity. For all other tested pre-cracked beams, where the matrix properties is modified (SFRC) or the severity of pre diagonal crack decreases (2.5 cm), the nonlinearity of the material is supreme to that of the geometrical effect, and as a result, the leading shear crack did not follow the geometry of pre-cracks.

According to the mode of failure of pre-cracked specimens tested in the present study, the leading shear crack for different beams occurred in three possible scenarios. **The 1st scenario** took place when the first shear crack appeared at the bottom of the pre-crack at a load similar to that of the control beam, then coalesced with the pre crack but still un-developed till reaching a higher load where multiple shear cracks formulate similar to that of the control beam at the stage of crack widening and propagation. At this point, the coalesced crack propagated to a main leading crack from the bottom to the far top of the beam. Although the length of propagated crack was suddenly increased due to coalescence with pre crack at lower load level, but it did not propagate at this level of load. The new formulated crack was kept stationary till reaching the proper load level for propagation. This behavior could be explained recalling fracture mechanics theory. A model for solving the fracture problem of RC beams was first proposed by (Carpinteri 1986), see Fig.7. The stress intensity factor, K, as a crack driving force, of the RC beam, KRC, was determined by two independent factors. The stress intensity factor, KM, due to the load applied at the middle of the cracked beam and the stress intensity factor, KF, due to the tensile force, FS, from the embedded reinforcing steel bar (closing force). Carpinteri estimated FS from the ultimate tensile or yield stresses of the steel bar. Baluch et al. (1992) assumed that the strain is linear along the depth of the RC beam and proportional to the distance measured from the neutral axis of the beam section. This improvement in Carpinteri's model provides a more realistic solution. Several investigators implemented the linear and non-linear fracture mechanics parameters to predict the crack propagation in RC beams Carpinteri et al (2014) and Fayyad and Lees (2017). As is already known, the fracture toughness of RC beams increased with increasing the crack length, not like monolithic materials. As the crack length increases the arm of the moment of FS increases, and subsequently, the closing effect of tensile reinforcement increases causing an increase of the fracture toughness of RC beams. This means that, for a certain cracked RC beam, the pre-crack with longer length needs higher initiation load than the shorter crack.

$$K = K_{RC} - K_S$$

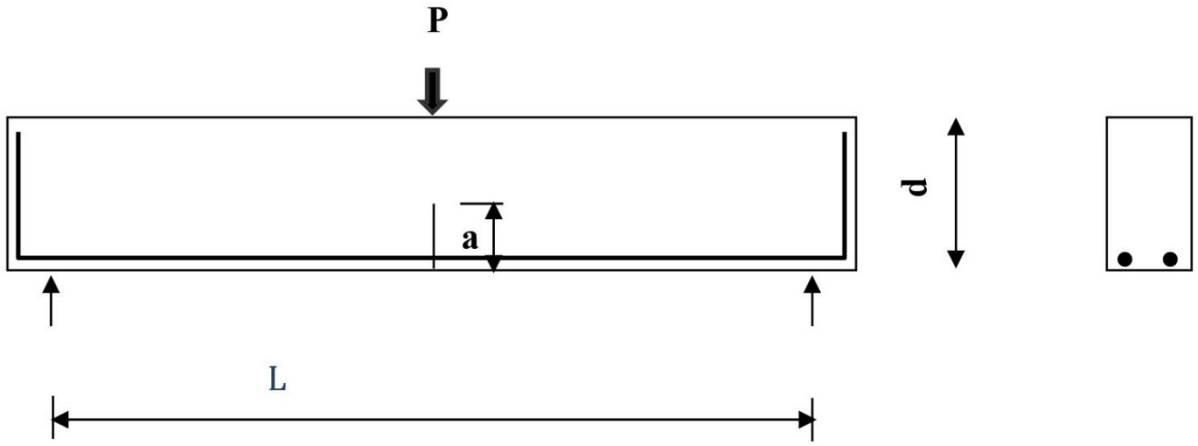

Fig.7*. Schematic drawing of a rectangular cracked RC beam*

This scenario was noticed for beams of HSC with crack lengths of 5.0 cm only (long crack) and different positions (Centered with and below the beam axis, P5C, P5SH) as shown in Fig. 5.

The 2nd scenario took place when the first shear crack appeared near by the pre-crack and propagated without coalescence with the pre-crack then widened and kinked toward the loading point and finally formulated a main leading crack neighbored to the pre-crack. This behavior was noticed in both plain high strength concrete with short cracks (2.5 cm) and SFRC beams with long crack and different position (P2.5C, P2.5SH, F5C, F5SH)as shown in Fig. 8.

The 3rd and last scenario took place when the first shear crack appeared at the un-cracked shear span of the beam then widened and propagated regardless the existence of a pre-crack on the opposite shear span. This behavior was noticed with SFRC beams with short crack and different position (F2.5C, F2.5SH) as shown in Fig. 9. The modes of failure in the 2nd and 3rd scenarios are more or less similar depending on the concrete heterogeneity rather than the existence of pre-crack.

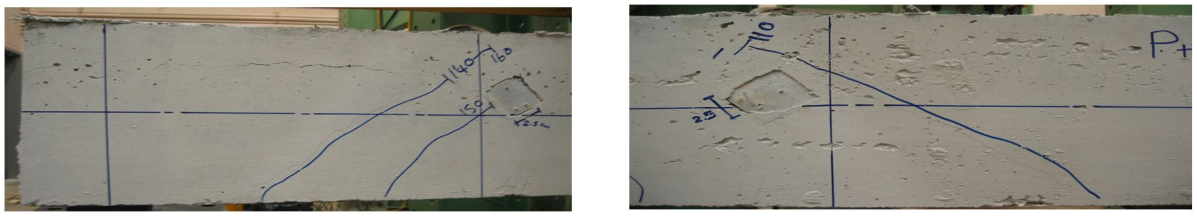

Figure 8: *Main shear crack neighbored to pre-Crack*

Figure 9: *Main shear crack at the other side of pre-crack*

The key word explaining these different scenarios is “Non Homogeneity”. Concrete with its variable sized particles from 0.5 to 20 mm exhibits a typical non homogeneous material. The presence of grain obstacles ahead of the crack dramatically affects its behavior. Kinking, branching, closure, and blunting are some of many other maneuvers could the crack face to avoid the for-headed obstacles. These situations might explain the first and second scenarios. Adding steel fibers as a new parameter to the concrete constituents adds more complexity. The randomization of steel fibers orientation related to the pre-crack direction makes the prediction of crack behavior

almost impossible. The pre-crack was formulated as a crack emanating from a notch root; the notch was fabricated as a pre-cast rubber latex strip embedded to the mold prior to casting. The existence of the rubber strip acts as a discontinuity plane of matrix, but it could gather steel fibers around its borders, making a fence of fibers in the predicted path of shear cracks, which might reveal the behavior in the third scenario of failure.

The relation between applied load and mid span deflection for all HSC beams with different pre-crack sizes and location is reported in Fig. 10. It is obvious from the figure that the P-δ curve behavior is insensitive to crack existence. Neither the size nor the location of crack affected the performance of beams. A similar behavior was found in SFRC beams as shown in Fig. 11. In previous investigations for the behavior of RC beams under mode I, Sallam et al (2004); Yehia and Wahab (2007), the behavior of p-δ curve of pre cracked specimen was typical to the smooth (un-cracked) specimen after the formulated crack reaches the length of the pre crack.

Another face of Non-homogeneity is expressed in Figs. 10 and 11. Although the pre-crack is embedded in the most favorable site and orientation, tested beams behaved blind as if no cracks exist in the element.

To study the role of each constituent parameter, strain gauges were fitted on main reinforcement, stirrups, and compression side of concrete as explained in the experimental program. Strain gauges readings versus applied load are reported in Figs. 12 to 14. It is clear that, stirrups in HSC beams suffer from yielding strain, and at the same load, stirrup in SFRC beams are still un-yielded due to the share of shear load resisted by steel fibers. However, Strains in stirrups for both concrete types were not affected by the location of main shear crack (the above three scenarios) as shown in Fig. 12.

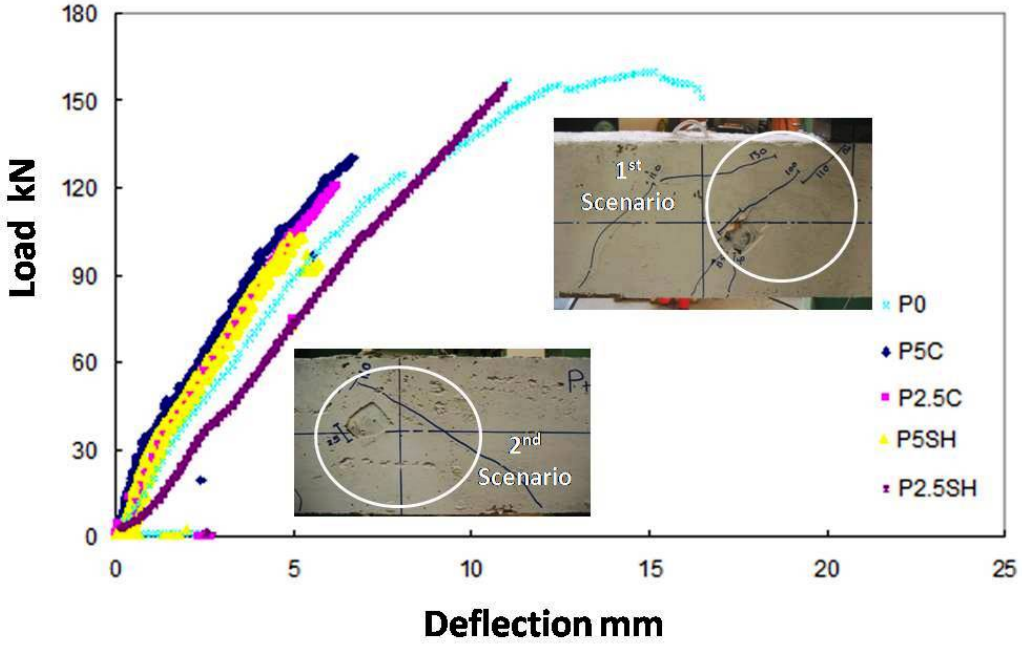

Figure 10: *Load Vs deflection (P-δ) for virgin and cracked HSC beams and Shear Cracks Patterns Scenarios*

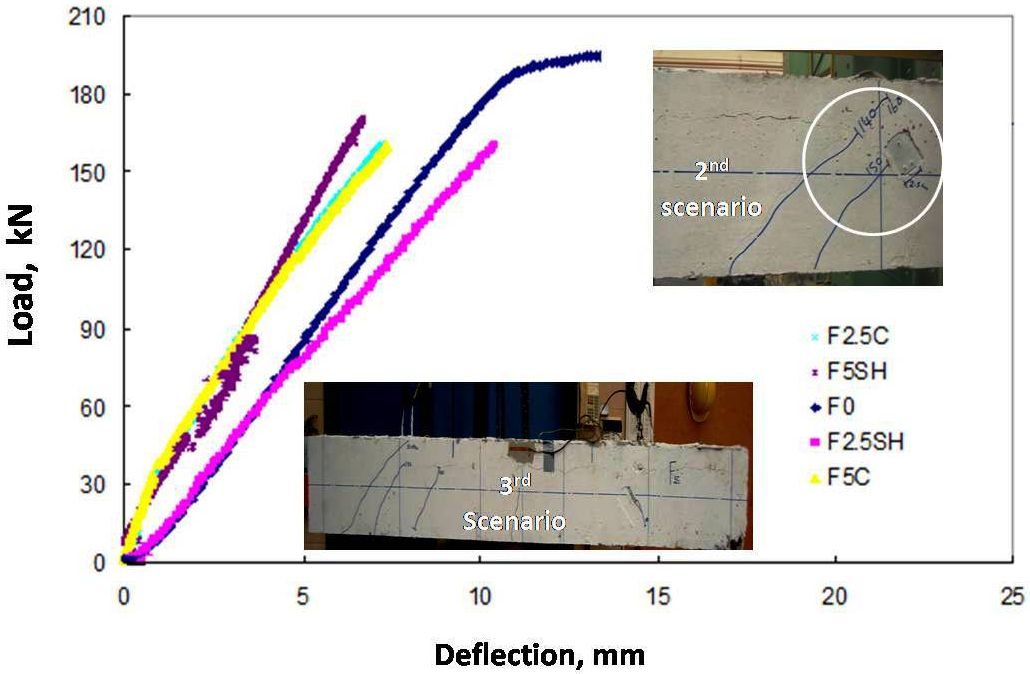

Figure 11: *Load Vs deflection (P-δ) for virgin and cracked SFRC beams and Shear Cracks Patterns Scenarios*

A similar behavior was noticed regarding strains on main reinforcement and strains on concrete compression zone. Neither of them was affected by the presence of pre-cracks. Moreover, the reported strain data reveals that the contribution of steel fibers is negligible in both tension and compression as shown in Figs. 13 and 14. All previous tools were un-sensitive to crack existence.

Due to the localization nature of crack initiation, Strain in Main Reinforcement, Strain in stirrups, strain in Compression zone of concrete, and over all behavior of the element represented in (P-δ) curve, all these parameters failed to predict the site of crack initiation in heterogeneous material, i.e. the resistance of material to both crack initiation and crack growth (R) varied from point to point. As is already known, the crack grows when the driving force (As strain energy release rate (G)) equals or exceeds (R)"$G \geq R$ and $\partial G/\partial a \geq \partial R/\partial a$". If the targeted material is homogeneous, the crack initiation and path could be easily predicted under the umbrella of fracture mechanics concepts.

The application of fracture mechanics concepts to predict shear behavior and failure mechanisms of reinforced concrete elements might be really promising. But the complexity of shear problem added to the existence of numerous variables and parameters stand as an obstacle to the success of such technique. In presence of cracks, whether they were originated while fabrication of element or generated under rising stresses, the shear behavior is greatly affected by their geometry. Geometrical variables of existed cracks such as, length, width, position and orientation in both two and three dimensions added to the element overall geometrical parameters such as, span to depth ratio, size effect, amount and position of reinforcement in both tension and compression, shear reinforcement, pattern and amount of stirrups, and orientation of such reinforcement are interacting together representing huge number of possibilities. All these parameters gathered to the non homogeneity of both plain and fiber reinforced concrete as a matrix made the problem really complex. Regarding the fact that, each combination of previously detailed parameters constitutes a unique case, then the applicability of fracture mechanics concepts to such a problem is too difficult and complex to be true.

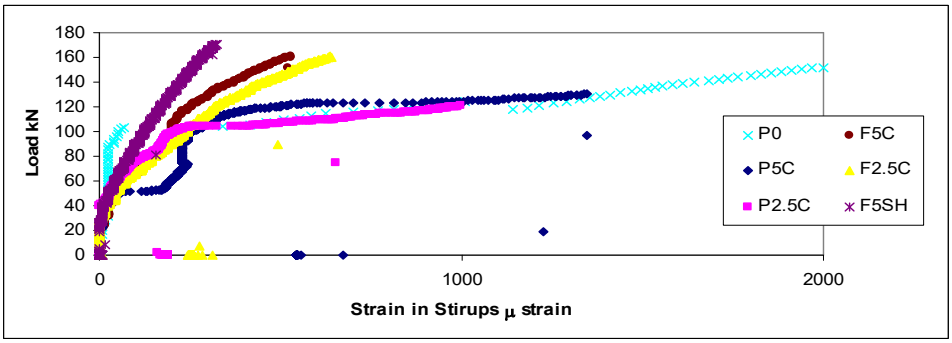

Figure 12: *Load Vs Strain in stirrups*

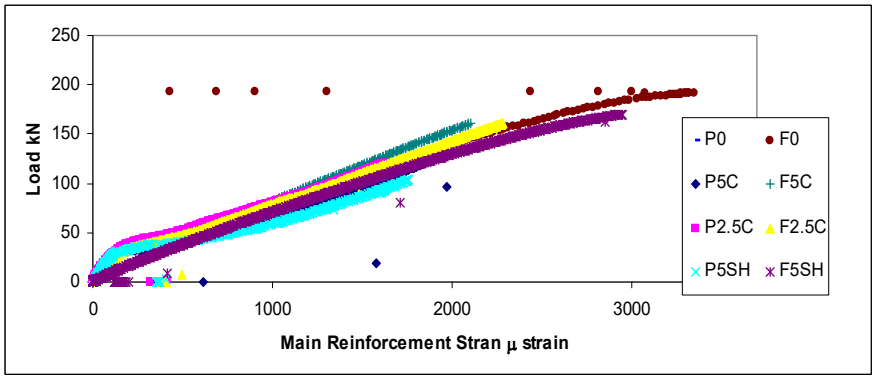

Figure 13: *Load Vs Strain in Main Reinforcement*

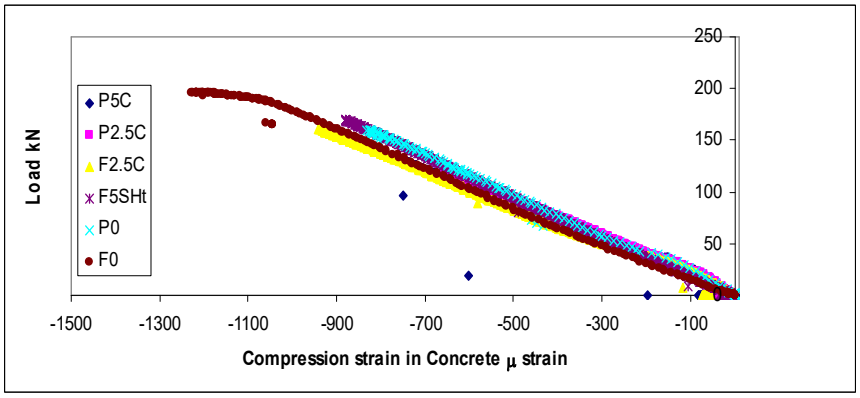

Figure 14: *Load Vs Compression Strain in Concrete.*

4 NUMERICAL STUDY

A numerical simulation was conducted to help in the verification of the experimental results. The main goal of this study was to ensure the behavior of shear and flexural cracks under the proposed loading system. To examine the geometrical effect of the pre-diagonal tension crack in shear span on the structural behavior of reinforced concrete beams, three dimensional finite element model has been constructed using ABAQUS/Standard code (ABAQUS 2007). All beam dimensions, and reinforcement types (tensile, compression, and shear) of the proposed experimental work have been taken into consideration as shown in Figs. 1 and 15. The materials were assumed to be elastic isotropic homogeneous material to consider only the geometrical effect without taking the material complexity effect into consideration. A general static analysis with displacement control was employed in the present study. Reinforced concrete beam was examined under symmetrical four point bend loading (4PB). The connection between the concrete and steel reinforcement was modeled as tie

constraint using master–slave surfaces in ABAQUS. The steel rebar was chosen as the master surface. The finite element meshes constructed with hexagonal structural mesh, C3D8R (8-node linear brick) elements, are used under Standard/static analysis.

In the present work, the domain integral method was used to extract stress intensity factors (SIFs) for reinforced concrete beams. In a finite element model SIF can be thought of as the virtual motion of a block of material surrounding each node along the crack line. Each such block is defined by contours: each contour is a ring of elements completely surrounding the nodes along the crack line from one crack face to the opposite crack face. These rings of elements are defined recursively to surround all previous contours.

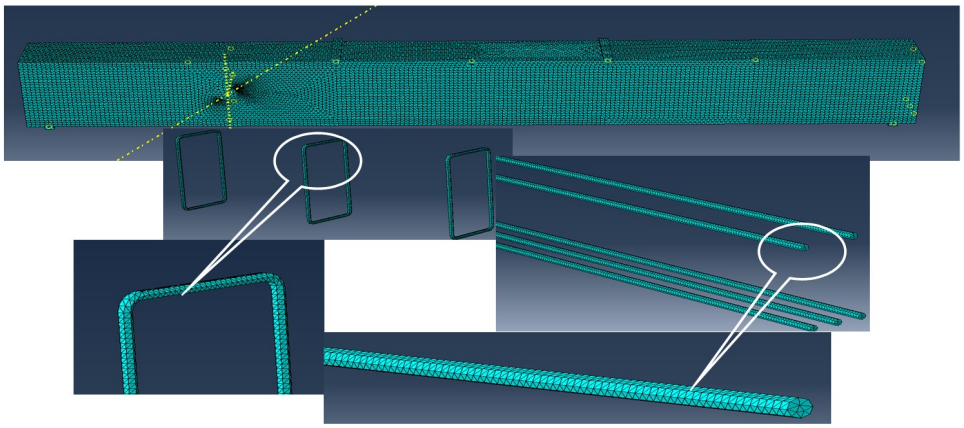

Figure 15: *Beam and Reinforcement Assembly of 3D Finite Element Modeling.*

ABAQUS/Standard automatically finds the elements that form each ring from the regions given as the crack-line definition. Each contour provides an evaluation of the contour integral. Using the divergence theorem, the contour integral can be expanded into a volume integral, over a finite domain surrounding the crack. This domain integral method is used to evaluate contour integrals in Abaqus/Standard. The method is quite robust in the sense that accurate contour integral estimates are usually obtained even with quite coarse meshes; because the integral is taken over a domain of elements surrounding the crack, errors in local solution parameters have less effect on the evaluated quantities such as the stress intensity factors. The stress intensity factors K_I, K_{II}, and K_{III}, (mode I, mode II and mode III SIF) are usually used in linear elastic fracture mechanics to characterize the local crack-tip/crack-line stress and displacement fields. They are related to the strain energy release rate (G) through

$$G = \frac{1}{8\pi} K^T B^{-1} K \tag{1}$$

Where $K = [K_I, K_{II}, K_{III}]^T$ and B is called the pre-logarithmic energy factor matrix, ABAQUS (2007) for homogeneous, isotropic materials B is diagonal and the above equation simplified to

$$G = \frac{1}{\bar{E}}\left(K_I^2 + K_{II}^2\right) + \frac{1}{2G} K_{III}^2 \tag{2}$$

Where $\bar{E} = E$ (E is modulus of elasticity) for plane stress and $\bar{E} = \dfrac{E}{\left(1-\nu^2\right)}$ (ν is Poisson's ratio) for plane strain, axisymmetry, and three dimension. The strain energy release rate is calculated directly in ABAQUS/Standard.

Strain energy release rate (G) was calculated for two different types of cracks (diagonal tension crack in shear span, and tensile crack in zero shear region) with different crack lengths. The distribution of shear stresses in different shear spans is shown in Fig. 16. It is clear from the figure that, the vicinity of pre-crack at the favorable site and orientation for shear failure concentrated the shear stresses around both crack tips.

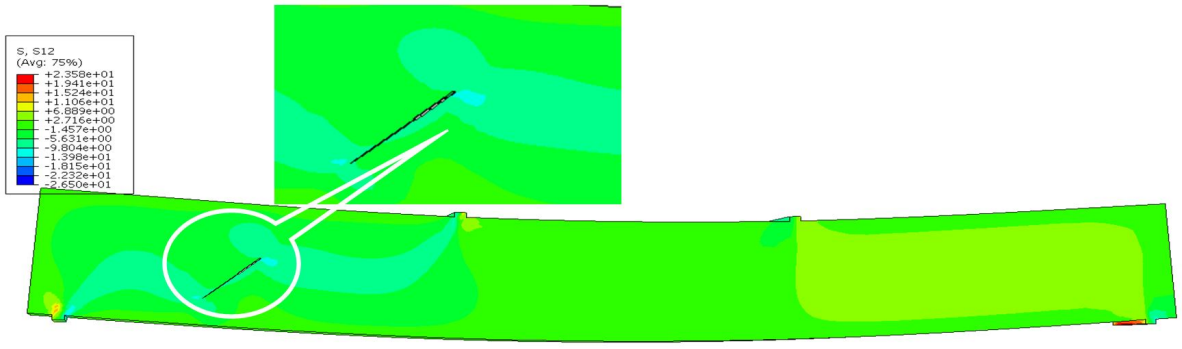

Figure 16: *Shear Fields Distribution in Vicinity of Pre-Crack.*

Figure 17 shows the relation between strain energy release rate (G) and crack length (a) for two types of cracks, at the same applied arbitrary load. For small crack length (≈ 20 mm) the driving force of the tensile crack is almost ten times the driving force of shear crack, which means that the tensile crack is the favorable type to grow that exceeding the critical strain energy release rate of the concrete (Gc). As expected the driving force of shear crack increases with increasing the crack length at the same applied load. On the other hand, with increasing length of tensile crack, the driving force G decreases markedly at the same applied load due to the closure effect of tensile reinforcement bars. As is already known, when the crack tip is away from the tensile reinforcement, the closuring moment of tensile reinforcement increases, and as a result reduces the strain energy release rate (G). Therefore, there is a certain long tensile crack has a driving force less than that of a short shear crack. For example at tensile crack of length 140 mm the driving force G is less than 0.5 N/mm while the driving force of 60 mm is higher than 0.5 N/mm as shown in Fig. 17. In accordance with the reported data of Abou El-Mal et al (2015a) previous research, tensile cracks grows to the load level of 110 kN for HSC beams and 140 kN for SFRC beams then shear cracks appears, at higher load levels the tensile cracks stop and the shear cracks keep propagating leading the failure mechanism to the end failure point.

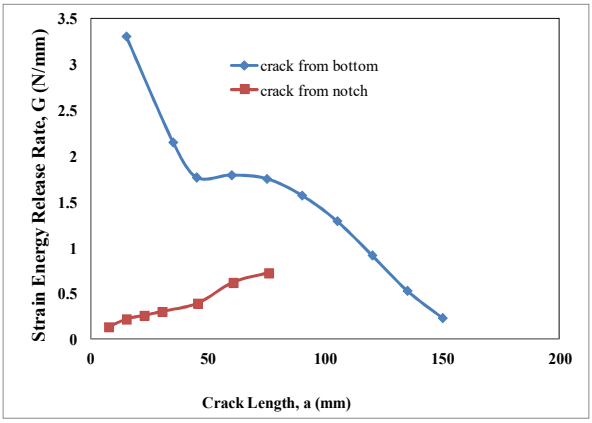

Figure 17: *Strain Energy Release Rate (G) Versus Crack Length (a).*

5 CONCLUSIONS

Based on the numerical and experimental results obtained from current study the following conclusions can be drawn:

1-The driving force of shear crack increases with increasing the crack length while, the driving force of tensile crack decreases markedly with increasing length of crack, at the same applied load due to the closure effect of the tensile reinforcement.

2- The path and behavior of the pre-cracked beam became identical to that of the control virgin beam after reaching 70.0 - 80.0% of the expected failure load for both HSC and SFRC tested beams, and consequently do not affect the ultimate shear strength of beams.

3- For HSC pre cracked beams with the most aggressive proposed pre-crack (the longer one 5.0cm) either centered with the beam axis denoted as (P5C) or totally located in the tension zone below the beam axis denoted as (P5SH).

4- According to the mode of failure of pre-cracked specimens tested in the present study, the leading shear crack for different beams occurred in three different scenarios regardless the size or the orientation of pre-crack. The leading shear crack whether coalesced or neighbored the pre-crack or appeared at the un-cracked shear span propagated at a load equal to that of smooth specimens at the same crack length.

5-Although surrounding constraints at maximum shear stress (at Neutral Axis) were released due to the presence of pre- cracks, the leading shear crack did not initiate at this zone, instead, it initiated from tension side then coalesced with the pre crack. This is due to, the weakness of concrete tensile strength in comparison to shear strength.

6-The crack closing effect increases with increasing the distance of the crack tip from the reinforcing steel in both tensile flexural cracks and diagonal tension shear cracks.

References

ABAQUS (2007) analysis user's manual. Version 6.7. Dassault Systèmes.

Abou El-Mal, H.S.S., Sherbini, A.S., Sallam, H.E.M. (2015a). Locating the site of diagonal tension crack initiation and path in reinforced concrete beams, Ain Shams Engineering Journal6: 17–24.

Abou El-Mal, H.S.S., Sherbini, A.S., Sallam, H.E.M. (2015b). Mode II Fracture Toughness of Hybrid FRCs, International Journal of Concrete Structures and Materials, 9: 475-486.

ACI Committee 318, (2005). Building Code Requirements for Reinforced Concrete (ACI 318-05) and Commentary, American Concrete Institute, Farmington Hills, MI, 430 pp.

ACI Committee Reports, ACI 446.1R-91, Reapproved (1999). Fracture Mechanics of Concrete, Concepts, Models and determination of Material Properties, Reported by ACI Committee 446, Fracture Mechanics, chaired by (Zdenek P. Bazant).

Baluch, M. H., Azad, A. K., Ashwavi, W., (1992). Fracture mechanics application to reinforced concrete members in flexure in Application of Fracture Mechanics to Reinforced Concrete, Carpinteri, A. (Ed.), London, pp. 413-436.

Bažant, Z. P., (1987). Fracture Energy of Heterogeneous Materials and Similitude, Fracture of Concrete and Rock, S. P. Shah and S. E. Swartz, 390-402.

Bažant, Z. P., (1984). Size Effect in Blunt Fracture: Concrete, Rock, Metal, Journal of Engineering Mechanics, ASCE 110: 518-35.

Bažant, Z. P., and Kim, J. K., (1984). Size Effect in Shear Failure of Longitudinal Reinforced Beams, ACI JOURNAL, Proceedings 81: 456-68.

Bažant, Z. P., and Yu, Q., (2005). Design against Size Effect on Shear Strength of Reinforced Concrete Beams without Stirrups," Journal of Structural Engineering, ASCE, 131: 1877-85.

BS 8110, (1997). Code of Practice for Design and Construction, Second edition, British Standards Institution, London, UK, 1-168.

Bykov, A. A., Matveenko, V. P., Serovaev, G. S., Shardakov, I. N., and Shestakov A. P. (2015). Analysis of the Influence of Dynamic Phenomena on the Fracture of a Reinforced Concrete Beam under Quasistatic Loading (Computations and Experiment) Mechanics of Solids, 50: 118-29.

Caldentey, A.P., Peiretti, H.C., Soto, A.G., and Iribarren, J.B. (2013). Cracking of RC members revisited: influence of cover, ϕ / $\rho_{s,ef}$ and stirrup spacing – an experimental and theoretical study", Structural Concrete, 14: 69-78.

Carpinteri A. Mechanical Damage and Crack Growth in Concrete. Martinus Nijhoff, Dordrecht, 1986.

Carpinteri A, Cadamuro E, Corrado M. (2014). Minimum flexural reinforcement in rectangular and T-section concrete beams. Structural Concrete, 15:361–372.

Carpinteri, A., Carmona, J. R., and Ventura, G. (2011). Failure Mode Transitions in Reinforced Concrete Beams, Part 1: Theoretical Model", ACI Structural Journal, 108: 277–85.

Chiu, C., Ueda, T., Chi, K., Chen, S. (2016). Shear Crack Control for High Strength Reinforced Concrete Beams Considering the Effect of Shear-Span to Depth Ratio of Member", International Journal of Concrete Structures and Materials 10: 407-24.

Coccia, S., Meda, A., and, Rinaldi, Z. (2015). On shear verification according to fib Model Code 2010 in FRC elements without traditional reinforcement, Structural Concrete, 16: 518-23.

Collins, M. P., (1978). Towards a rational theory for RC members in shear, J. Struct. Div. ASCE 104: 649- 66.

CSA Committee A23.3 (1994). Design of Concrete Structures: Structures (Design) A National Standard of Canada, Canadian standards Association, Rexdale, ON, Canada, 199 pp.

Fayyad, T.M. and Lees, J.M. (2017). Experimental investigation of crack propagation and crack branching in lightly reinforced concrete beams using digital image correlation. Engineering Fracture Mechanics, 182: 487–505.

Gastebled, O. J., and May, I. M., (2001). Fracture Mechanics Model Applied to Shear Failure of Reinforced Concrete Beams without Stirrups, ACI Structural Journal, 98: 184-90.

Gustafsson, P. J., and Hillerborg, A., (1988). Sensitivity in Shear Strength of Longitudinally Reinforced Concrete Beams ACI Structural Journal 85: 286-94.

Jenq, Y. S., and Shah, S. P., (1989). Shear Resistance of Reinforced Concrete Beams—A Fracture Mechanics Approach Fracture Mechanics: Application to Concrete, SP-118, V. Li and Z. P. Bažant, eds., American Concrete Institute, Farmington Hills, MI, 237-258.

Kani, G.N.J., (1966). Basic Facts Concerning Shear Failure, ACI, J Proc 63: 675-92.

Kani, G.N.J., (1964). The Riddle of Shear Failure and Its Solution, Journal of ACI 61:441-67.

Kotsovos, M. D., (1988). Compressive force path concept: basis for reinforced concrete ultimate limit design', ACI Struct. J. 85: 68-75.

Lim, W., Hong, S. (2016). Shear Tests for Ultra-High Performance Fiber Reinforced Concrete (UHPFRC) Beams with Shear Reinforcement", International Journal of Concrete Structures and Materials 10: 177-88.

Reinhardt, H. W., (1981). Size Effect on Shear Tests in the Light of Fracture Mechanics, Beton- und Stahlbetonbau 76: 19-21.

Resende, T.L., Shehata, L.C.D., Shehata, I.A. (2016). Shear strength of self-compacting concrete beams with small amounts of stirrups", Structural Concrete 17:3-10.

Sagaseta, J. (2013). The influence of aggregate fracture on the shear strength of reinforced concrete beams: an experimental and analytical research project", Structural Concrete 14: 401-14.

Sallam, H.E.D.M., Mubaraki, M., Yusoff, N.I.M. (2014). Application of the maximum undamaged defect size (dmax) concept in fiber-reinforced concrete pavements, Arab. J. Sci. Eng. 39: 8499-506.

Sallam, H.E.M., Saba, A.M., Shaheen, H.H., and Abdel-Raouf, H. (2004). Prevention of peeling failure in plated beams, J. Adv. Concr.Technol., JCI 2: 419-429.

Schlaich, J., Sch/ifer, K. and Jennewein, M., (1987) Toward a consistent design of structural concrete, Prestr. Concr. Inst. J. 32: 74-150.

So, K. O., and Karihaloo, B. L., (1993). Shear Capacity of Longitudinally Reinforced Beams—A Fracture Mechanics Approach, ACI Structural Journal 90: 591-600.

Swartz, S. E., Hu, K. K., and Jones, G. L. (1978). Compliance Monitoring of Crack Growth in Concrete, J. of the Engng. Mech. Div., ASCE, 104: 789-800.

Vecchio, F. J. and Collins, M. P., (1986). The modified compression-field theory for reinforced concrete elements subjected to shear, ACI Struct. J. 83: 219-31.

Yehia, N.A.B., Wahab, N.M. (2007). Fracture mechanics of flanged reinforced concrete sections, Engineering Structures 29: 2334–43.